

# Odd Elasticity of a Catalytic Micromachine

Akira Kobayashi,<sup>1</sup> Kento Yasuda,<sup>2</sup> Kenta Ishimoto,<sup>2</sup> Li-Shing Lin,<sup>1</sup> Isamu Sou,<sup>1</sup> Yuto Hosaka,<sup>3</sup> and Shigeyuki Komura<sup>4,5,1,\*</sup>

<sup>1</sup>*Department of Chemistry, Graduate School of Science, Tokyo Metropolitan University, Tokyo 192-0397, Japan*

<sup>2</sup>*Research Institute for Mathematical Sciences, Kyoto University, Kyoto 606-8502, Japan*

<sup>3</sup>*Max Planck Institute for Dynamics and Self-Organization (MPI DS), Am Fassberg 17, 37077 Göttingen, Germany*

<sup>4</sup>*Wenzhou Institute, University of Chinese Academy of Sciences, Wenzhou, Zhejiang 325001, China*

<sup>5</sup>*Oujiang Laboratory, Wenzhou, Zhejiang 325000, China*

We perform numerical simulations of a model micromachine driven by catalytic chemical reactions. Our model includes a mechano-chemical coupling between the structural variables and the nonequilibrium variable describing the catalytic reactions. The time-correlation functions of the structural variables are calculated and further analyzed in terms of odd Langevin dynamics. We obtain the effective odd elastic constant that manifests the broken time-reversal symmetry of a catalytic micromachine. Within the simulation, we separately estimate the quantity called nonreciprocity and show that its behavior is similar to that of the odd elasticity. Our approach suggests a new method to extract the nonequilibrium properties of a micromachine only by measuring its structural dynamics.

## I. INTRODUCTION

In recent years, the physics of micromachines such as bacteria, motor proteins, and artificial molecular machines has been intensively studied [1–3]. A micromachine can be defined as a small object that extracts energy from chemical substances in the system and further exhibits mechanical functions [4, 5]. The interplay between the structural dynamics of such a small object and associated chemical reaction is crucial for biological functions of a micromachine [6–8]. Owing to the developments in nonequilibrium statistical mechanics and experimental techniques, various research has been conducted to reveal the energetics of a single micromachine [9–12].

In our previous work, we proposed a model that describes cyclic state transitions of a micromachine driven by catalytic chemical reactions [13]. As we shall explain later, we considered a mechano-chemical coupling of the variables representing the chemical reaction and the internal structural state of a micromachine. To estimate the functionality of a micromachine, we focused on the physical quantity called “nonreciprocity” that represents the area enclosed by a trajectory in the conformational space. Such a quantity directly determines the average velocity of a three-sphere microswimmer [14–16] or the crawling speed of a cell on a substrate [17, 18].

Recently, Scheibner *et al.* introduced the concept of odd elasticity that is useful to characterize nonequilibrium active systems [19, 20]. Odd elasticity arises from antisymmetric (odd) components of the elastic modulus tensor that violates the energy conservation law and thus can exist only in active materials [21, 22] or biological systems [23]. Recently, some of the present authors proposed a thermally driven microswimmer with odd elastic-

ity and demonstrated that it can exhibit a directional locomotion [24, 25]. The concept of odd elasticity was also applied to Purcell’s three-link swimmer model [26] and to robotic systems [27]. We also showed that antisymmetric parts of the time-correlation functions in odd Langevin systems are proportional to the odd elasticity [28, 29]. Whilst many theoretical models are proposed to explain microscopic physical origins of odd elasticity, quantitative measurements of the odd elastic modulus are still lacking in these stochastic and nonequilibrium systems.

In this paper, we perform extensive numerical simulations of a model micromachine driven by catalytic chemical reactions [13]. We calculate the time-correlation functions of the structural variables and analyze them in terms of effective even and odd elasticity of coupled Langevin equations [28]. Importantly, the presence of odd elasticity reflects the broken time-reversal symmetry of a catalytic micromachine. We also show that the nonreciprocity is proportional to the odd elasticity in the current stochastic model. Our approach provides us with a new method to extract the nonequilibrium properties of a micromachine only by measuring its structural dynamics without invoking the dynamics of the chemical reaction [30].

The current work is based on our previous two papers in Refs. [13] and [28], and further completes our general view on stochastic micromachines. In these works, we explicitly discuss the effects of thermal fluctuations which provide driving forces for micromachines. One of the results specific to our stochastic system is that the average work is proportional to the square of the odd elastic constant (see Sec. III D) [24]. It should be also emphasized that the concept of odd elasticity is not limited to elastic materials. Although we focus on catalytic micromachines, most of the results also apply to general odd stochastic systems such as the odd microswimmer [28, 29]. In our previous paper in Ref. [13], we solved our model almost analytically by using several approxi-

\* komura@wiucas.ac.cn

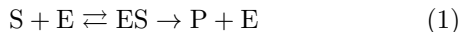
mations. In this work, on the other hand, we numerically solve the same equations in the presence of noise without using any crude approximations. Such a study is necessary for the complete understanding of the proposed model.

In Sec. II, we briefly review our model of a micromachine driven by a catalytic chemical reaction and explain the numerical method [13]. In Sec. III, we show the results of the numerical simulations and discuss the properties of the time-correlation functions [28]. Then we estimate effective even and odd elastic constants by using the result of the overdamped odd Langevin equations. A summary of our work and some discussion are given in Sec. IV.

## II. CATALYTIC MICROMACHINE

### A. Model

We first explain our model of a catalytic micromachine which was introduced in Ref. [13] and is schematically shown in Fig. 1(a). Consider a system which contains one enzyme molecule (E) that acts as a micromachine, substrate molecules (S), and product molecules (P). The enzyme molecule plays the role of a catalyst and the corresponding chemical reaction is written as [31]



where ES indicates a complex molecule. In our model, we introduce a dimensionless reaction variable  $\theta(t)$  to quantify the extent of the catalytic reaction. The reaction variable  $\theta$  is a continuous number and increases  $2\pi$  for each reaction.

According to the Kramers theory, the free energy  $G_r$  describing a chemical reaction is given by a tilted periodic potential [32]

$$G_r(\theta) = -A \cos \theta - F\theta, \quad (2)$$

as schematically represented in Fig. 1(b). The first term is a periodic potential with a period of  $2\pi$  and  $A$  is the energy barrier. This is because  $\theta$  increases by  $2\pi$  for one cycle of chemical reaction and should experience the same potential. On the other hand,  $F$  in Eq. (2) represents the chemical potential difference that drives catalytic reaction. For example,  $F$  represents the chemical potential change before and after ATP hydrolysis.

Next, we introduce the dimensionless state variables  $s_i(t)$  ( $i = 1, 2, 3, \dots$ ) characterizing the conformation of a micromachine. As shown in Fig. 1(a), examples of the state variables are distances between the domains in a micromachine. To introduce the mechano-chemical coupling mechanism, we assume that each state variable  $s_i$  experiences a harmonic potential,  $(C_i/2)[s_i - \ell_i(\theta)]^2$ , where  $C_i$  is the coupling parameter and  $\ell_i(\theta)$  is the dimensionless natural state that depends on the reaction variable  $\theta$ . We consider that the natural state  $\ell_i(\theta)$

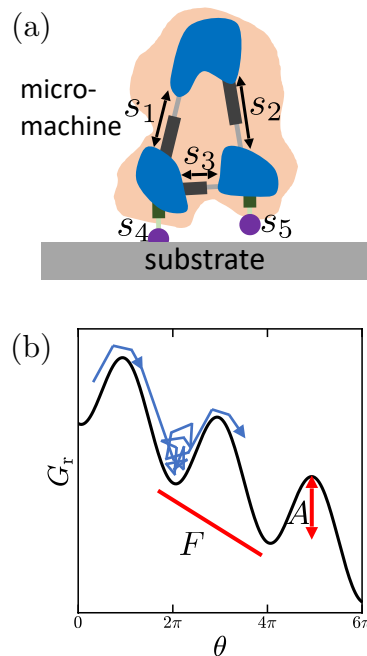


FIG. 1. (Color online) (a) Schematic picture of a micromachine characterized by the conformational state variables  $s_1$ ,  $s_2$ , and  $s_3$ . Moreover, the adhesion between the domains and the substrate is described by the variables  $s_4$  and  $s_5$ . (b) The tilted periodic potential  $G_r(\theta)$ , where  $\theta$  is the catalytic reaction variable. As expressed in Eq. (2),  $A$  is the energy barrier and  $F$  corresponds to the nonequilibrium force. A possible trajectory of  $\theta$  is schematically shown by the blue arrow. The value of  $\theta$  fluctuates around the minimum of the potential and the transition to the next minimum takes place occasionally. Reprinted figure with permission from Ref. [13]. Copyright (2021) by the American Physical Society.

changes periodically and assume the simplest periodic form  $\ell_i(\theta) = \sin(\theta + \phi_i)$ , where  $\phi_i$  is the constant phase difference relative to the reaction phase  $\theta$  [33, 34]. Under these assumptions, we consider the following mechano-chemical coupling energy  $G_c$  between  $\theta$  and  $s_i$ :

$$G_c(\theta, \{s_i\}) = \sum_i \frac{C_i}{2} [s_i - \sin(\theta + \phi_i)]^2. \quad (3)$$

Then the total free energy  $G_t$  in our model is simply given by

$$G_t(\theta, \{s_i\}) = G_r(\theta) + G_c(\theta, \{s_i\}). \quad (4)$$

For the time evolution of  $\theta$  and  $s_i$ , we employ the Onsager's phenomenological equations in the presence of noises [35, 36]

$$\dot{\theta} = -\mu_\theta \frac{\partial G_t}{\partial \theta} + \xi_\theta(t), \quad (5)$$

$$\dot{s}_i = -\sum_j \mu_{ij} \frac{\partial G_t}{\partial s_j} + \xi_i(t), \quad (6)$$

where dot indicates the time derivative. In the above equations, the time-evolutions of the variables are proportional to the respective thermodynamic forces, and they relax to the thermal equilibrium state for which the total free energy is minimized. Here,  $\mu_\theta$  and  $\mu_{ij}$  are the mobility coefficients, and  $\xi_\theta$  and  $\xi_i$  represent thermal fluctuations which satisfy the following fluctuation-dissipation theorem [35, 36]

$$\langle \xi_\theta(t) \rangle = 0, \quad \langle \xi_\theta(t) \xi_\theta(t') \rangle = 2\mu_\theta k_B T \delta(t - t'), \quad (7)$$

$$\langle \xi_i(t) \rangle = 0, \quad \langle \xi_i(t) \xi_j(t') \rangle = 2\mu_{ij} k_B T \delta(t - t'), \quad (8)$$

$$\langle \xi_\theta(t) \xi_i(t') \rangle = 0, \quad (9)$$

where  $k_B$  is the Boltzmann constant and  $T$  is the temperature.

Although our model is general and includes many degrees of freedom, we make several simplifications to capture the physical insight of a catalytic micromachine. First, we only consider two degrees of freedom, i.e.,  $s_1$  and  $s_2$ . Second, the mobility coefficients  $\mu_{ij}$  ( $i, j = 1, 2$ ) is assumed to have the form  $\mu_{ij} = \mu_s \delta_{ij}$ , where  $\delta_{ij}$  is the Kronecker delta. Third, the coupling free energy is symmetric between the two degrees of freedom, i.e.,  $C_1 = C_2 = C$ . In this work, we investigate the case when  $\phi_1 = 0$  because different choices of  $\phi_1$  give qualitatively the same  $\phi_2$ -dependence. Then Eqs. (5) and (6) reduce to the following simplified set of equations [13]

$$\begin{aligned} \dot{\theta} = & -\mu_\theta [A \sin \theta - F - C \cos \theta [s_1 - \sin \theta] \\ & - C \cos(\theta + \phi_2) [s_2 - \sin(\theta + \phi_2)]] + \xi_\theta, \end{aligned} \quad (10)$$

$$\dot{s}_1 = -\mu_s C [s_1 - \sin \theta] + \xi_1, \quad (11)$$

$$\dot{s}_2 = -\mu_s C [s_2 - \sin(\theta + \phi_2)] + \xi_2. \quad (12)$$

Notice that the above equations are difficult to solve analytically because they are highly nonlinear although some attempts were made in Ref. [13].

## B. Numerical method

In the above model, the variables  $\theta$  and  $s_i$  are dimensionless, whereas  $A$ ,  $F$ , and  $C$  have the dimension of energy. The latter quantities are all scaled by the thermal energy  $k_B T$  and the corresponding dimensionless quantities are defined by  $\hat{A} = A/(k_B T)$ ,  $\hat{F} = F/(k_B T)$ , and  $\hat{C} = C/(k_B T)$ , respectively. The dimensionless time is defined by  $\hat{t} = 2\mu_\theta k_B T t$  and the ratio between the two mobilities is fixed to  $\mu_s/\mu_\theta = 1$  in our simulation.

We numerically solve the coupled stochastic differential equations in Eqs. (10)–(12) by integrating the following dimensionless quantities

$$\begin{aligned} d\theta = & (\hat{F} - \hat{A} \sin \theta) d\hat{t} + \hat{C} \cos \theta [s_1 - \sin \theta] d\hat{t} \\ & + \hat{C} \cos(\theta + \phi_2) [s_2 - \sin(\theta + \phi_2)] d\hat{t} + dW_\theta, \end{aligned} \quad (13)$$

$$ds_1 = -\hat{C} [s_1 - \sin \theta] d\hat{t} + dW_1, \quad (14)$$

$$ds_2 = -\hat{C} [s_2 - \sin(\theta + \phi_2)] d\hat{t} + dW_2, \quad (15)$$

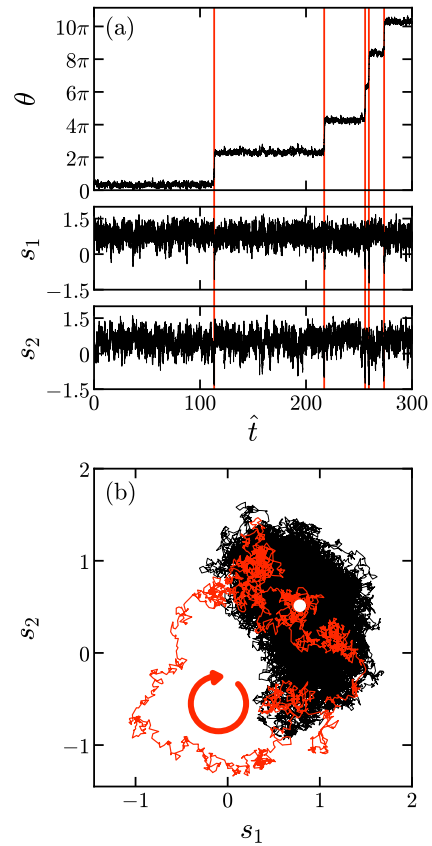


FIG. 2. (Color online) (a) Time evolution of  $\theta$ ,  $s_1$ , and  $s_2$  as a function of dimensionless time  $\hat{t} = 2\mu_\theta k_B T t$  when  $\hat{A} = 20$ ,  $\hat{F} = 16$ ,  $\hat{C} = 20$ ,  $\phi_2 = \pi/2$ , and  $\mu_s/\mu_\theta = 1$ . The red vertical lines indicate the moments when the catalytic chemical reactions take place. (b) The trajectory of  $s_1$  and  $s_2$  corresponding to one cycle of chemical reaction that occurs in (a). When  $\theta$  fluctuates around the local minimum of the potential energy  $G_r(\theta)$ ,  $s_1$  and  $s_2$  also fluctuate (black trajectory for  $115 \leq \hat{t} < 216.5$ ) around the average position (white circle). When the chemical reaction takes place and  $\theta$  changes by  $2\pi$ , the trajectory forms a closed loop (red trajectory for  $112.5 \leq \hat{t} < 115$ ) in a clockwise manner as shown by the red circular arrow.

where  $dW_\theta, dW_1, dW_2 \sim \sqrt{dt}$  are the increment of Wiener processes.

When we numerically calculate the statistical average  $\langle X \rangle$  of a quantity  $X$ , we use the long-time average. This is justified because we have checked that the ensemble average and the time average give the same result in our simulation after the system reaches the steady state.

## III. SIMULATION RESULTS

### A. Time evolution

As an example of the simulation result, we show in Fig. 2(a) the time evolution of  $\theta$  (top),  $s_1$  (middle), and

$s_2$  (bottom) for certain set of parameters. When the catalytic reaction occurs, we see that the reaction variable  $\theta$  increases in a stepwise manner by  $2\pi$ , whereas the state variables  $s_1$  and  $s_2$  undergo almost random fluctuations. Corresponding to the occasional increase of  $\theta$ , both  $s_1$  and  $s_2$  tend to show peaks as indicated by the vertical red lines. Although the result in Fig. 2(a) demonstrates that the present model micromachine is indeed driven by thermal fluctuations, it is difficult to isolate the peaks of  $s_i$  because they are almost comparable to the background fluctuations. Moreover, the state transitions become very rare when  $\hat{A} \gg 1$ .

In Fig. 2(b), we plot a typical trajectory of  $s_1$  and  $s_2$  for one typical cycle of chemical reaction. While  $\theta$  fluctuates around the local minimum,  $s_1$  and  $s_2$  also fluctuate (black trajectory) around the average structure specified by the white circle. When  $\theta$  increases by  $2\pi$ , the trajectory of  $s_1$  and  $s_2$  follows a directional closed loop (red trajectory). The direction is clockwise when  $0 < \phi_2 < \pi$  (as shown by the red arrow) or counterclockwise when  $\pi < \phi_2 < 2\pi$ . The area enclosed by the trajectory can be obtained by the following quantity called “nonreciprocity” [13]

$$R_{12} = \oint dt \dot{s}_1 s_2, \quad (16)$$

where the integral is taken over one cycle. The statistical property of  $R_{12}$  in our stochastic simulation will be discussed later in Sec. III D. (We avoid to use the terminology “nonreciprocity” that has broader and general meanings [37–39].)

## B. Time-correlation functions

From the time series of  $s_1$  and  $s_2$  in Fig. 2(a), we calculate the structural time-correlation functions of a catalytic micromachine. We first define the time-dependent fluctuation by  $x_i(t) = s_i(t) - \langle s_i \rangle$ , where  $\langle s_i \rangle$  is the average of  $s_i$ . Then the matrix of time-correlation functions  $\phi_{ij}(t)$  is defined as

$$\phi_{ij}(t) = \langle x_i(t)x_j(0) \rangle = \phi_{ij}^S(t) + \phi_{ij}^A(t). \quad (17)$$

In the above,  $\phi_{ij}(t)$  is decomposed into the symmetric and antisymmetric parts which satisfy  $\phi_{ij}^S(t) = \phi_{ji}^S(t)$  and  $\phi_{ij}^A(t) = -\phi_{ji}^A(t)$ , respectively [28]. For our later purpose, we also define the equal-time-correlation functions with a bar as  $\bar{\phi}_{ij} = \phi_{ij}(0)$ .

When the system is in equilibrium for which the time-reversal symmetry holds, the correlation functions must satisfy the reciprocal relation  $\phi_{ij}^{\text{eq}}(t) = \phi_{ji}^{\text{eq}}(t)$  for  $i \neq j$  [35, 36]. This is equivalent to saying that the antisymmetric part of the correlation function  $\phi_{ij}^A(t)$  should vanish in equilibrium [28]. In nonequilibrium situations, however, the antisymmetric parts can exist because the time-reversal symmetry can be generally violated [40–42].

In Fig. 3(a), we plot both the self-correlation functions  $\phi_{11}(t)$  (black) and  $\phi_{22}(t)$  (red) as a function of the

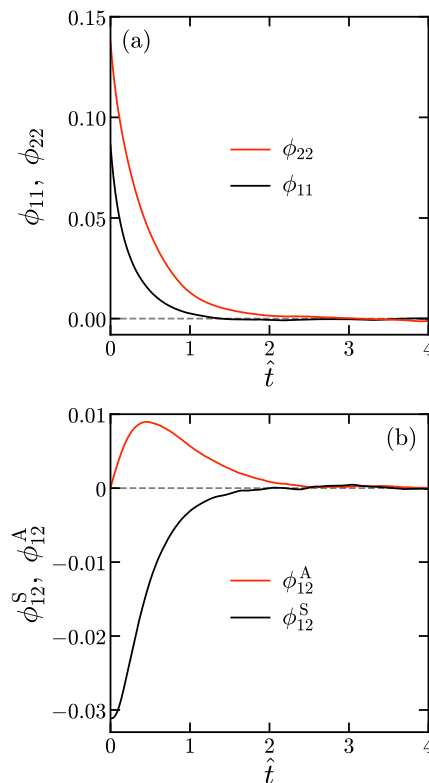


FIG. 3. (Color online) (a) The self-correlation functions  $\phi_{11}(t)$  (black) and  $\phi_{22}(t)$  (red) as a function of the dimensionless time  $\hat{t}$ . (b) The symmetric part of the cross correlation function  $\phi_{12}^S(t) = [\phi_{12}(t) + \phi_{21}(t)]/2$  (black) and the antisymmetric part of the cross correlation function  $\phi_{12}^A(t) = [\phi_{12}(t) - \phi_{21}(t)]/2$  (red) as a function of the dimensionless time  $\hat{t}$ . For both (a) and (b), the parameters are the same as in Fig. 2.

dimensionless time  $\hat{t}$ . The overall behavior of the self-correlation functions is nearly described by an exponential function with a slight modification. Although the equal-time-correlation functions  $\bar{\phi}_{11}$  and  $\bar{\phi}_{22}$  take different values, the slopes of the initial decay are the same for these self-correlation functions. Notice that the initial decay of the correlation function reflects the mobility of the system.

In Fig. 3(b), we plot both the symmetric part of the cross correlation function  $\phi_{12}^S(t) = [\phi_{12}(t) + \phi_{21}(t)]/2$  (black) and the antisymmetric part of the cross correlation function  $\phi_{12}^A(t) = [\phi_{12}(t) - \phi_{21}(t)]/2$  (red) as a function of  $\hat{t}$ . We clearly see that  $\phi_{12}^A(t)$  is nonzero, namely,  $\phi_{12}(t) \neq \phi_{21}(t)$  for  $0 < \hat{t} < 2$ . This means that the time-reversal symmetry is explicitly broken and hence the antisymmetric part of the cross-correlation function exists in the present catalytic system. As we discuss below, the antisymmetric parts of the correlation functions can be quantitatively characterized by effective odd elasticity [28].

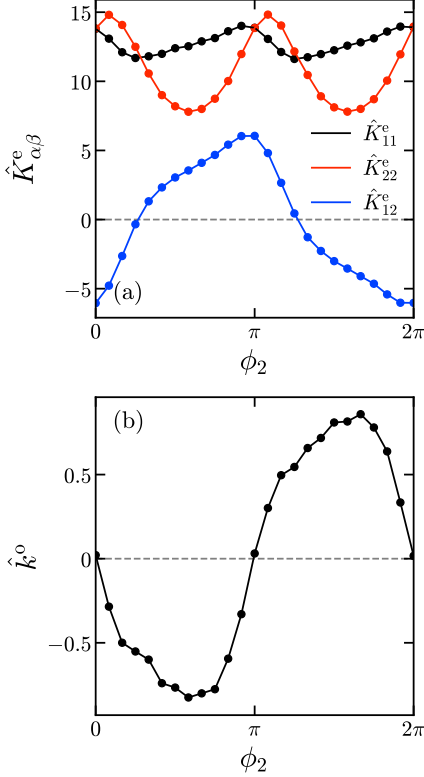


FIG. 4. (Color online) (a) The dimensionless effective even elastic constants  $\hat{K}_{11}^e = K_{11}^e/(k_B T)$  (black),  $\hat{K}_{22}^e = K_{22}^e/(k_B T)$  (red), and  $\hat{K}_{12}^e = K_{12}^e/(k_B T)$  (blue) as a function of the phase difference  $\phi_2$ . (b) The dimensionless effective odd elastic constant  $\hat{k}^o = k^o/(k_B T)$  as a function of  $\phi_2$ . For both (a) and (b), the other parameters are the same as in Fig. 2.

### C. Effective even and odd elastic constants

The short-time behaviors of the obtained correlation functions have the following characteristic features; (i) the initial slopes of the self-correlation functions  $\phi_{11}(t)$  and  $\phi_{22}(t)$  are the same, (ii) the initial slope of the symmetric part of the cross correlation function  $\phi_{12}^S(t)$  vanishes, i.e.,  $\dot{\phi}_{12}^S(0) = 0$ , (iii) the initial value of the antisymmetric part of the cross correlation function  $\bar{\phi}_{12}^A$  vanishes, i.e.,  $\bar{\phi}_{12} = \bar{\phi}_{21}$ .

Under these conditions, the obtained correlation functions can be interpreted in terms of the following coupled odd Langevin equations:

$$\dot{x}_1 = -\mu(K_{11}x_1 + K_{12}x_2) + \zeta_1, \quad (18)$$

$$\dot{x}_2 = -\mu(K_{21}x_1 + K_{22}x_2) + \zeta_2, \quad (19)$$

where  $\mu$  is the effective mobility and  $\zeta_\alpha$  ( $\alpha = 1, 2$ ) is Gaussian white noise that satisfies the fluctuation dissipation relation. More general situations and the statistical property of the noises were discussed in Ref. [28]. The effective elastic constant matrix  $K_{\alpha\beta}$  can be written in terms of even and odd elastic constants as follows [see

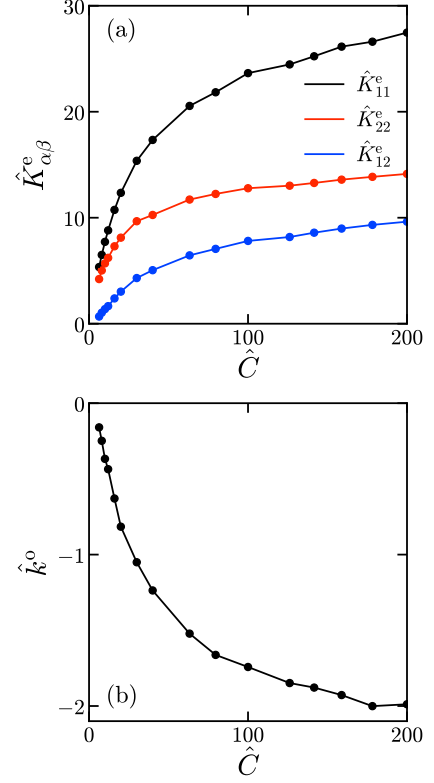


FIG. 5. (Color online) (a) The dimensionless effective even elastic constants  $\hat{K}_{11}^e$  (black),  $\hat{K}_{22}^e$  (red), and  $\hat{K}_{12}^e$  (blue) as a function of the dimensionless coupling parameter  $\hat{C} = C/(k_B T)$ . (b) The dimensionless effective odd elastic constant  $\hat{k}^o$  as a function of  $\hat{C}$ . For both (a) and (b), the other parameters are the same as in Fig. 2.

Eqs. (A4) and (A5)]

$$\begin{pmatrix} K_{11} & K_{12} \\ K_{21} & K_{22} \end{pmatrix} = \begin{pmatrix} K_{11}^e & K_{12}^e + k^o \\ K_{12}^e - k^o & K_{22}^e \end{pmatrix}, \quad (20)$$

where  $K_{11}^e$ ,  $K_{12}^e$ , and  $K_{22}^e$  are even elastic constants and  $k^o$  is the odd elastic constant [19, 24, 29].

In Appendix A, we show that the short-time behaviors of the symmetric and antisymmetric parts of the correlation functions obtained from Eqs. (18) and (19) are given by [see Eqs. (A11) and (A12)]

$$\phi_{\alpha\beta}^S(t) \approx \bar{\phi}_{\alpha\beta} - k_B T \mu |t| \delta_{\alpha\beta}, \quad (21)$$

$$\phi_{\alpha\beta}^A(t) \approx -\frac{2k^o k_B T \mu t}{\text{tr}[K^e]} \epsilon_{\alpha\beta}, \quad (22)$$

where  $\text{tr}[K^e]$  is the trace of the matrix  $K_{\alpha\beta}^e$  and  $\epsilon_{\alpha\beta}$  is the 2D Levi-Civita tensor. The equal-time-correlation function  $\bar{\phi}_{\alpha\beta}$  in Eq. (21) is now given by [see Eq. (A10)]

$$\begin{aligned} \bar{\phi}_{\alpha\beta} = & \frac{k_B T}{1 + \nu^2} \left[ ((K^e)^{-1})_{\alpha\beta} + \frac{2\nu^2}{\text{tr}[K^e]} \delta_{\alpha\beta} \right. \\ & \left. + \frac{k^o}{\det[K^e] \text{tr}[K^e]} (\epsilon_{\alpha\gamma} K_{\gamma\beta}^e + \epsilon_{\beta\gamma} K_{\gamma\alpha}^e) \right], \quad (23) \end{aligned}$$

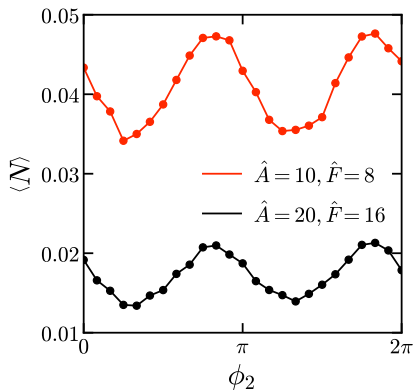


FIG. 6. (Color online) The average number of reaction cycle per unit time  $\langle N \rangle$  as a function of the phase difference  $\phi_2$  when  $\hat{A} = 20$  and  $\hat{F} = 16$  (black) and when  $\hat{A} = 10$  and  $\hat{F} = 8$  (red). The other parameters are the same as in Fig. 2.

where  $\det[K^e]$  is the determinant of  $K_{\alpha\beta}^e$ ,  $((K^e)^{-1})_{\alpha\beta}$  is the inverse of  $K_{\alpha\beta}^e$ , and  $\nu^2 = (k^\circ)^2 / \det[K^e]$ . Using these expressions, we extract the effective even and odd elastic constants of the catalytic micromachine. We first checked that  $\mu/\mu_\theta \approx 1.0$  holds in the simulation, which is consistent with the choice of the parameter  $\mu_s/\mu_\theta = 1$ . Hence we can identify  $\mu$  with  $\mu_s$  and obtain the effective elastic constants.

In Fig. 4(a), we plot the three dimensionless even elastic constants  $\hat{K}_{\alpha\beta}^e = K_{\alpha\beta}^e / (k_B T)$  as a function of the phase difference  $\phi_2$ . We see that they are periodic function of  $\phi_2$ . The period of  $K_{11}^e$  and  $K_{22}^e$  is  $\pi$ , whereas that of  $K_{12}^e$  is  $2\pi$ . In Fig. 4(b), on the other hand, we plot  $\hat{k}^\circ = k^\circ / (k_B T)$  as a function of  $\phi_2$ . Notice that  $k^\circ$  can take negative values and roughly approximated as  $k^\circ \sim -\sin \phi_2$ . The present analysis implies that the effective elasticity (both even and odd) can be obtained only by measuring the structural dynamics without knowing any detailed dynamics of the chemical reaction variable  $\theta$ .

In Figs. 5(a) and (b), on the other hand, we plot  $\hat{K}_{\alpha\beta}^e$  and  $\hat{k}^\circ$ , respectively, as a function of the coupling parameter  $\hat{C}$  while the phase difference is fixed to  $\phi_2 = \pi/2$ . We see in Fig. 5(a) that the even elastic constants  $K_{\alpha\beta}^e$  increase with  $C$ . Although the sign of the odd elastic constant  $k^\circ$  is negative in Fig. 5(b), its magnitude also increases when  $C$  is made larger.

#### D. Nonreciprocity and power efficiency

To characterize the nonequilibrium degree of a micro-machine, it is useful to consider the nonreciprocity defined in Eq. (16). For the current stochastic model, we first discuss the average number of reaction cycle per unit time that is obtained by dividing the total number of cycles by the total simulation time. In Fig. 6, we

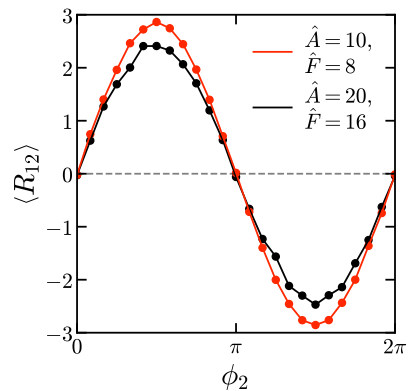


FIG. 7. (Color online) The average nonreciprocity  $\langle R_{12} \rangle$  as a function of  $\phi_2$  when  $\hat{A} = 20$  and  $\hat{F} = 16$  (black) and when  $\hat{A} = 10$  and  $\hat{F} = 8$  (red). The other parameters are the same as in Fig. 2.

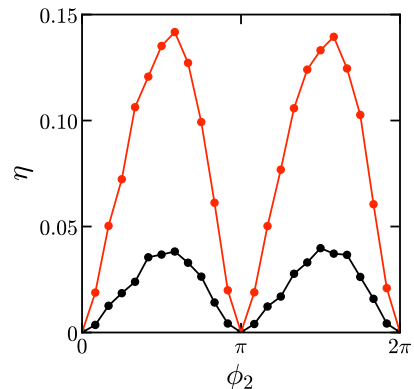


FIG. 8. (Color online) The power efficiency  $\eta = \langle W \rangle / (2\pi F)$  as a function of the phase difference  $\phi_2$  when  $\hat{A} = 20$  and  $\hat{F} = 16$  (black) and when  $\hat{A} = 10$  and  $\hat{F} = 8$  (red). The other parameters are the same as in Fig. 2.

plot  $\langle N \rangle$  as a function of the phase difference  $\phi_2$  for two combinations of  $A$  and  $F$  values. We find that  $\langle N \rangle$  is a periodic function of  $\phi_2$  and the period is  $\pi$ .

Next, we calculate the statistical average of nonreciprocity  $R_{12}$  over many cycles of chemical reaction. To do so, we accumulate the quantity  $\dot{s}_1 s_2$  over long time and divide it by the total number of cycles during the simulation to obtain  $\langle R_{12} \rangle$  per one cycle which is plotted in Fig. 7 as a function of  $\phi_2$ . We see that the behavior of  $\langle R_{12} \rangle$  is similar to that of  $k^\circ$  in Fig. 4(b) and can be approximated as  $\langle R_{12} \rangle \sim \sin \phi_2$ . This result is reasonable because it was shown before that  $\langle R_{12} \rangle$  is given by the time derivative of Eq. (22) and can be written as [26]

$$\langle R_{12} \rangle = -\frac{2k^\circ k_B T \mu}{\text{tr}[K^e] \langle N \rangle}, \quad (24)$$

where  $\langle N \rangle^{-1}$  is the average period of the reaction cycle. This expression confirms that  $\langle R_{12} \rangle$  is proportional to  $k^\circ$ . Hence the average nonreciprocity  $\langle R_{12} \rangle$  becomes

nonzero only if there is finite odd elasticity. We note again that such dynamics occur when the elastic constants are nonreciprocal, i.e.,  $K_{12} \neq K_{21}$  in Eq. (20).

The presence of odd elasticity indicates that mechanical work is done by the micromachine through its structural change and the average work per unit cycle is given by [19]

$$\langle W \rangle = -2k^\circ \langle R_{12} \rangle. \quad (25)$$

In Fig. 8, we plot the average power efficiency defined by  $\eta = \langle W \rangle / (2\pi F)$  as a function of the phase difference  $\phi_2$  by using the simulation result. Notice that the energy supplied during one cycle of the catalytic reaction is  $2\pi F$ . The power efficiency vanishes when  $\phi_2 = 0, \pi$ , and  $2\pi$  for which the deformation of the micromachine is reciprocal. This is also reasonable because if we substitute Eq. (24) into Eq. (25) the average work should approximately behave as [24]

$$\langle W \rangle \sim (k^\circ)^2 \sim (\sin \phi_2)^2. \quad (26)$$

We also find that the power efficiency increases when the activation energy  $A$  and the nonequilibrium driving force  $F$  become smaller. Hence the micromachine can have a higher  $\eta$  value when thermal fluctuations are larger compared with the potential barrier.

#### IV. SUMMARY AND DISCUSSION

In this paper, we have performed numerical simulations of a model micromachine driven by catalytic chemical reactions as previously proposed by some of the present authors [13]. We have obtained the structural time-correlation functions and also extracted their symmetric and antisymmetric parts (see Fig. 3). These results were further analyzed in terms of odd Langevin dynamics and we have obtained the effective even and odd elastic constants of the catalytic system (see Figs. 4 and 5). The presence of the odd elasticity demonstrates the broken time-reversal symmetry and we have confirmed that the nonreciprocity  $\langle R_{12} \rangle$  is proportional to the odd elastic constant  $k^\circ$  (see Fig. 7). We have also calculated the power efficiency of a micromachine and found that it increases when the activation energy  $A$  becomes smaller (see Fig. 8).

Let us summarize here our perspectives on stochastic micromachines, which have been discussed in our previous papers [13, 28] as well as in this work that completes our view. First, the concept of odd elasticity is not necessarily limited to elastic materials as in the original work [19] but can also be applied to general nonreciprocal systems with odd interactions. Second, we have explicitly discussed the role of thermal fluctuations in catalytic micromachines and showed that the average work is proportional to the square of the odd elastic constant [see Eq. (26)]. Third, we have suggested how to extract nonequilibrium properties of a micromachine

only by measuring its structural dynamics even when the chemical reaction variable is a hidden nonequilibrium variable.

Recently, we have derived dynamical equations for a nonequilibrium active system with odd elasticity by using Onsager's variational principle [30]. We showed that the elimination of an extra variable that is coupled to the nonequilibrium driving force leads to the nonreciprocal set of equations for the structural coordinates [43]. The obtained nonreciprocal equations manifest the physical origin of the odd elastic constants that are proportional to the nonequilibrium force and the friction coefficients [19]. In the present work, the reaction variable  $\theta(t)$  is driven by the nonequilibrium force  $F$  and coupled to the structural variables  $s_i$ . Similar to Ref. [30], the elimination of the nonequilibrium variable results in the nonreciprocal deformation of a micromachine characterized by  $R_{12}$  in Eq. (16). This explains how a micromachine converts chemical energy to mechanical work and such a mechanism can be common for proteins, enzymes, and even microswimmers [24, 25].

We have analyzed the time-correlation functions of a catalytic micromachine in terms of overdamped Langevin equations with odd elasticity as shown in Eq. (A1). In Appendix A, we have assumed that the corresponding mobility matrix  $M_{\alpha\beta}$  is symmetric, i.e.,  $M_{\alpha\beta} = M_{\beta\alpha}$ , according to Onsager's reciprocal relation [36]. If we remove this assumption and if  $M_{\alpha\beta}$  is not symmetric, one also needs to consider the odd viscosity [44]. Odd viscosity accounts for the fluid flow perpendicular to the velocity gradient and does not contribute to energy dissipation [45–48]. Hence, odd viscosity needs to be taken into account when the surrounding environment of a micromachine is in out-of-equilibrium situations. In such cases, however, we cannot rely on the fluctuation dissipation relation that we have used in the derivation of the correlation functions [28].

Finally, we discuss some typical values of the parameters used in our numerical simulations and evaluate the effective odd elastic constant. According to the experiments on F<sub>1</sub>-ATPase, the activation energy and the chemical potential difference can be roughly estimated as  $A \approx 10 k_B T$  [11] and  $F \approx 3 k_B T$  [10]. Using the relation for work per cycle  $\langle W \rangle = 2\pi F \eta$  as in the previous section, we estimate  $\langle W \rangle \approx 2 k_B T$  when  $\eta \approx 0.1$  (see Fig. 8). We shall further identify this work as  $\langle W \rangle \sim \kappa^\circ d^2$ , where  $\kappa^\circ$  is the odd elastic constant in unit of J/m<sup>2</sup> ( $k^\circ$  in this paper has the dimension of energy) and  $d \approx 10^{-8}$  m is the typical enzyme size [28]. Then one can roughly estimate as  $\kappa^\circ \approx 10^{-4}$  J/m<sup>2</sup>, which is also consistent with our previous estimate for a kinesin molecule [28].

#### ACKNOWLEDGMENTS

K.Y. acknowledges the support by a Grant-in-Aid for JSPS Fellows (No. 22KJ1640) from the Japan Society for the Promotion of Science (JSPS). K.I. acknowl-

edges the JSPS, KAKENHI for Transformative Research Areas A (No. 21H05309) and the Japan Science and Technology Agency (JST), PRESTO Grant (No. JP-MJPR1921). K.Y. and K.I. were supported by the Research Institute for Mathematical Sciences, an International Joint Usage/Research Center located in Ky-

oto University. S.K. acknowledges the support by the National Natural Science Foundation of China (Nos. 12274098 and 12250710127) and the startup grant of Wenzhou Institute, University of Chinese Academy of Sciences (No. WIUCASQD2021041). A.K. and K.Y. contributed equally to this work.

### Appendix A: Time-correlation functions for odd Langevin systems

In this Appendix, we briefly review the results of the time-correlation functions for odd Langevin systems [28]. As shown in Fig. 1(a), we consider a deformable object such as an enzyme in a passive viscous fluid. We investigate its dynamics driven by the energy injection owing to catalytic chemical reactions. For this purpose, we consider an overdamped Langevin system with an odd elastic tensor. The Langevin equation for the state variables  $x_\alpha(t)$  ( $\alpha = 1, 2, 3, \dots$ ) can be written as [35, 36, 49–51]

$$\dot{x}_\alpha = -M_{\alpha\beta}K_{\beta\gamma}x_\gamma + \zeta_\alpha, \quad (\text{A1})$$

where  $M_{\alpha\beta}$  is the mobility tensor that is symmetric, i.e.,  $M_{\alpha\beta} = M_{\beta\alpha}$ , due to Onsager's reciprocal relation [35, 36]. Moreover,  $M_{\alpha\beta}$  is positive definite according to the second law of thermodynamics. In Eq. (A1),  $\zeta_\alpha$  is Gaussian white noise that has following statistical properties:

$$\langle \zeta_\alpha(t) \rangle = 0, \quad \langle \zeta_\alpha(t)\zeta_\beta(t') \rangle = 2D_{\alpha\beta}\delta(t-t'), \quad (\text{A2})$$

where  $D_{\alpha\beta}$  is the diffusion tensor and satisfies the fluctuation dissipation relation  $D_{\alpha\beta} = k_B T M_{\alpha\beta}$  [35, 36]. The equal-time-correlation function  $\bar{\phi}_{\alpha\beta} = \langle x_\alpha x_\beta \rangle$  obeys the Lyapunov equation [49–51]:

$$M_{\alpha\gamma}K_{\gamma\delta}\bar{\phi}_{\delta\beta} + M_{\beta\gamma}K_{\gamma\delta}\bar{\phi}_{\delta\alpha} = 2D_{\alpha\beta}. \quad (\text{A3})$$

In Eq. (A1),  $K_{\alpha\beta}$  is the elastic constant tensor. For active systems with nonconservative interactions,  $K_{\alpha\beta}$  can have an antisymmetric part that corresponds to the odd elasticity [19, 24, 29]. Hence,  $K_{\alpha\beta}$  can generally be written as

$$K_{\alpha\beta} = K_{\alpha\beta}^e + K_{\alpha\beta}^o, \quad (\text{A4})$$

where the symmetric (even) part and the antisymmetric (odd) part satisfy  $K_{\alpha\beta}^e = K_{\beta\alpha}^e$  and  $K_{\alpha\beta}^o = -K_{\beta\alpha}^o$ , respectively. We further consider a system with only two degrees of freedom ( $\alpha, \beta = 1, 2$ ) and assume that the elastic tensor is given by the following form:

$$K_{\alpha\beta} = K_{\alpha\beta}^e + k^o \epsilon_{\alpha\beta}, \quad (\text{A5})$$

where  $k^o$  is the scalar odd elastic constant and  $\epsilon_{\alpha\beta}$  is the 2D Levi-Civita tensor with  $\epsilon_{11} = \epsilon_{22} = 0$  and  $\epsilon_{12} = -\epsilon_{21} = 1$ .

In our previous paper [28], we showed that the equal-time-correlation function when  $\alpha, \beta = 1, 2$  becomes

$$\bar{\phi}_{\alpha\beta} = \frac{k_B T}{1 + \nu^2} \left[ ((K^e)^{-1})_{\alpha\beta} + \frac{2\nu^2}{\text{tr}[MK^e]} M_{\alpha\beta} - \frac{k^o \det[M]}{\text{tr}[MK^e]} [\epsilon_{\alpha\gamma}(M^{-1})_{\gamma\delta}((K^e)^{-1})_{\delta\beta} + \epsilon_{\beta\gamma}(M^{-1})_{\gamma\delta}((K^e)^{-1})_{\delta\alpha}] \right], \quad (\text{A6})$$

where “tr” and “det” indicate the trace and determinant of the matrix, respectively,  $((K^e)^{-1})_{\alpha\beta}$  is the inverse of  $K_{\alpha\beta}^e$ , and  $\nu^2 = (k^o)^2 / \det[K^e]$  (see Eq. (C2) in Ref. [28]). The above expression can be rewritten as

$$\bar{\phi}_{\alpha\beta} = \frac{k_B T}{1 + \nu^2} \left[ ((K^e)^{-1})_{\alpha\beta} + \frac{2\nu^2}{\text{tr}[MK^e]} M_{\alpha\beta} + \frac{k^o}{\det[K^e]\text{tr}[MK^e]} [\epsilon_{\alpha\gamma}K_{\gamma\delta}^e M_{\delta\beta} + \epsilon_{\beta\gamma}K_{\gamma\delta}^e M_{\delta\alpha}] \right]. \quad (\text{A7})$$

In the short-time limit, the time-correlation function can be decomposed into the symmetric and antisymmetric parts as  $\phi_{\alpha\beta}(t) = \phi_{\alpha\beta}^S(t) + \phi_{\alpha\beta}^A(t)$ , and they are respectively given by

$$\phi_{\alpha\beta}^S(t) \approx \bar{\phi}_{\alpha\beta} - k_B T M_{\alpha\beta} |t|, \quad (\text{A8})$$

$$\phi_{\alpha\beta}^A(t) \approx -\frac{2k^o k_B T \det[M] t}{\text{tr}[MK^e]} \epsilon_{\alpha\beta}, \quad (\text{A9})$$



(see Eq. (C6) in Ref. [28]).

According to our simulation results, the mobility matrix can be further simplified as  $M_{\alpha\beta} = \mu\delta_{\alpha\beta}$ . In this case, Eqs. (A7), (A8), and (A9) further become

$$\bar{\phi}_{\alpha\beta} = \frac{k_{\text{B}}T}{1 + \nu^2} \left[ ((K^e)^{-1})_{\alpha\beta} + \frac{2\nu^2}{\text{tr}[K^e]} \delta_{\alpha\beta} + \frac{k^o}{\det[K^e]\text{tr}[K^e]} (\epsilon_{\alpha\gamma} K_{\gamma\beta}^e + \epsilon_{\beta\gamma} K_{\gamma\alpha}^e) \right], \quad (\text{A10})$$

$$\phi_{\alpha\beta}^{\text{S}}(t) \approx \bar{\phi}_{\alpha\beta} - k_{\text{B}}T\mu|t|\delta_{\alpha\beta}, \quad (\text{A11})$$

$$\phi_{\alpha\beta}^{\text{A}}(t) \approx -\frac{2k^o k_{\text{B}}T\mu t}{\text{tr}[K^e]} \epsilon_{\alpha\beta}. \quad (\text{A12})$$

These expressions are used to extract the effective elastic constants of a catalytic micromachine.

- 
- [1] S. Toyabe and M. Sano, *J. Phys. Soc. Jpn.* **84**, 102001 (2015).
- [2] C. Bechinger, R. Di Leonardo, H. Löwen, C. Reichhardt, G. Volpe, and G. Volpe, *Rev. Mod. Phys.* **88**, 045006 (2016).
- [3] A. I. Brown and D. A. Sivak, *Chem. Rev.* **120**, 434 (2020).
- [4] K. K. Dey, F. Wong, A. Altemose, and A. Sen, *Curr. Opin. Colloid Interface Sci.* **21**, 4 (2016).
- [5] Y. Hosaka and S. Komura, *Biophys. Rev. Lett.* **17**, 51 (2022).
- [6] Y. Togashi, T. Yanagida, and A. S. Mikhailov, *PLoS Comput. Biol.* **6**, e1000814 (2010).
- [7] M. L. Mugnai, C. Hyeon, M. Hinczewski, and D. Thirumalai, *Rev. Mod. Phys.* **92**, 025001 (2020).
- [8] Y. Hosaka, S. Komura, and A. S. Mikhailov, *Soft Matter* **16**, 10734 (2020).
- [9] T. Harada and S.-i. Sasa, *Phys. Rev. Lett.* **95**, 130602 (2005).
- [10] S. Toyabe, T. Okamoto, T. Watanabe-Nakayama, H. Taketani, S. Kudo, and E. Muneyuki, *Phys. Rev. Lett.* **104**, 198103 (2010).
- [11] R. Hayashi, K. Sasaki, S. Nakamura, S. Kudo, Y. Inoue, H. Noji, and K. Hayashi, *Phys. Rev. Lett.* **114**, 248101 (2015).
- [12] T. Ariga, M. Tomishige, and D. Mizuno, *Phys. Rev. Lett.* **121**, 218101 (2018).
- [13] K. Yasuda and S. Komura, *Phys. Rev. E* **103**, 062113 (2021).
- [14] R. Golestanian and A. Ajdari, *Phys. Rev. E* **77**, 036308 (2008).
- [15] I. Sou, Y. Hosaka, K. Yasuda, and S. Komura, *Phys. Rev. E* **100**, 022607 (2019).
- [16] I. Sou, Y. Hosaka, K. Yasuda, and S. Komura, *Physica A* **562**, 125277 (2021).
- [17] M. Leoni and P. Sens, *Phys. Rev. Lett.* **118**, 228101 (2017).
- [18] M. Tarama and R. Yamamoto, *J. Phys. Soc. Jpn.* **87**, 044803 (2018).
- [19] C. Scheibner, A. Souslov, D. Banerjee, P. Surówka, W. T. Irvine, and V. Vitelli, *Nat. Phys.* **16**, 475 (2020).
- [20] M. Fruchart, C. Scheibner, and V. Vitelli, *Annu. Rev. Condens. Matter Phys.* **14**, 471 (2023).
- [21] D. Zhou and J. Zhang, *Phys. Rev. Res.* **2**, 023173 (2020).
- [22] L. Braverman, C. Scheibner, B. VanSaders, and V. Vitelli, *Phys. Rev. Lett.* **127**, 268001 (2021).
- [23] T. H. Tan, A. Mietke, J. Li, Y. Chen, H. Higinbotham, P. J. Foster, S. Gokhale, J. Dunkel, and N. Fakhri, *Nature* **607**, 287 (2022).
- [24] K. Yasuda, Y. Hosaka, I. Sou, and S. Komura, *J. Phys. Soc. Jpn.* **90**, 075001 (2021).
- [25] A. Kobayashi, K. Yasuda, L.-S. Lin, I. Sou, Y. Hosaka, and S. Komura, *J. Phys. Soc. Jpn.* **92**, 034803 (2023).
- [26] K. Ishimoto, C. Moreau, and K. Yasuda, *Phys. Rev. E* **105**, 064603 (2022).
- [27] M. Brandenbourger, C. Scheibner, J. Veenstra, V. Vitelli, and C. Coulais, arXiv:2108.08837
- [28] K. Yasuda, K. Ishimoto, A. Kobayashi, L.-S. Lin, I. Sou, Y. Hosaka, and S. Komura, *J. Chem. Phys.* **157**, 095101 (2022).
- [29] K. Yasuda, A. Kobayashi, L.-S. Lin, Y. Hosaka, I. Sou, and S. Komura, *J. Phys. Soc. Jpn.* **91**, 015001 (2022).
- [30] L.-S. Lin, K. Yasuda, K. Ishimoto, Y. Hosaka, and S. Komura, *J. Phys. Soc. Jpn.* **92**, 033001 (2023).
- [31] K. Dill and S. Bromberg, *Molecular Driving Forces: Statistical Thermodynamics in Biology, Chemistry, Physics, and Nanoscience* (Garland Science, London and New York, 2010).
- [32] P. Hänggi, P. Talkner, and M. Borkovec, *Rev. Mod. Phys.* **62**, 251 (1990).
- [33] A. S. Mikhailov and R. Kapral, *Proc. Natl. Acad. Sci. USA* **112**, E3639 (2015).
- [34] J. Agudo-Canalejo, T. Adeleke-Larodo, P. Illien, and R. Golestanian, *Phys. Rev. Lett.* **127**, 208103 (2021).
- [35] R. Kubo, M. Toda, and N. Hashitsume, *Statistical Physics II* (Springer, New York, 1991).
- [36] M. Doi, *Soft Matter Physics* (Oxford University Press, Oxford, 2013).
- [37] C. Caloz, A. Alù, S. Tretyakov, D. Sounas, K. Achouri, and Z.-L. Deck-Léger, *Phys. Rev. Applied* **10**, 047001 (2018).
- [38] H. Nassar, B. Yousefzadeh, R. Fleury, M. Ruzzene, A. Alù, C. Daraio, A. N. Norris, G. Huang, M. R. Haberman, *Nat. Rev. Mater.* **5**, 667 (2020).
- [39] D. Zhou, D. Z. Rocklin, M. Leamy, and Y. Yao, *Nat. Commun.* **13**, 3379 (2022).
- [40] J. M. Epstein and K. K. Mandadapu, *Phys. Rev. E* **101**,

- 052614 (2020).
- [41] C. Hargus, K. Klymko, J. M. Epstein, and K. K. Mandadapu, *J. Chem. Phys.* 152, 201102 (2020).
  - [42] M. Han, M. Fruchart, C. Scheibner, S. Vaikuntanathan, J. J. de Pablo, and V. Vitelli, *Nat. Phys.* 17, 1260 (2021).
  - [43] M. Fruchart, R. Hanai, P. B. Littlewood, and V. Vitelli, *Nature* 592, 363 (2021).
  - [44] J. E. Avron, *J. Stat. Phys.* 92, 543 (1998).
  - [45] D. Banerjee, A. Souslov, A. G. Abanov, and V. Vitelli, *Nat. Commun.* 8, 1573 (2017).
  - [46] Y. Hosaka, S. Komura, and D. Andelman, *Phys. Rev. E* 103, 042610 (2021).
  - [47] Y. Hosaka, S. Komura, and D. Andelman, *Phys. Rev. E* 104, 064613 (2021).
  - [48] Y. Hosaka, D. Andelman, and S. Komura, *Eur. Phys. J. E* 46, 18 (2023).
  - [49] J. B. Weiss, *Tellus A* 55, 208 (2003).
  - [50] J. B. Weiss, *Phys. Rev. E* 76, 061128 (2007).
  - [51] J. B. Weiss, B. Fox-Kemper, D. Mandal, A. D. Nelson, and R. K. P. Zia, *J. Stat. Phys.* 179, 1010 (2020).